A novel particle swarm optimisation technique to improve energy efficiency of doubly-fed induction generators for wind turbines

Sompracha, Cherngchai; Jayaweera, Dilan; Tricoli, Pietro

A novel particle swarm optimisation technique to improve energy efficiency of doubly-fed induction generators for wind turbines

C Sompracha*, D Jayaweera*, P Tricoli*

**Department of Electronic, Electrical and Systems Engineering, University of Birmingham, Birmingham, United Kingdom*

Email: CXS407@student.bham.ac.uk; D.Jayaweera@bham.ac.uk; P.Tricoli@bham.ac.uk

Keywords: Maximum power point tracking, model-based loss minimisation control, particle swarm optimisation, wind energy conversion system.

Abstract

Wind energy conversion systems requires a suitable control to maximise the power generated by wind turbines independently on the wind conditions. Variable-speed fixed-pitch wind turbines with doubly-fed induction generators are used in WECSs for their higher reliability and efficiency compared to variable-pitch wind turbine systems. This paper proposes an effective control algorithm to maximise the efficiency of fixed-pitch wind turbines with doubly-fed induction generators using particle swarm optimization control to compensate for the errors in the estimation of the circuit parameters of the generator. The proposed control algorithm generates an optimal speed reference to optimise the mechanical power extracted from the wind and the optimal *d*-axis rotor current through stator reactive power management to minimise the electrical losses of the doubly-fed generator. The optimal speed reference is provided by a maximum power point tracking control below the rated wind speed and a soft-stalling control above the rated wind speed, while the optimal *d*-axis rotor current is searched by a particle swarm optimisation algorithm. The proposed control system has been verified by numerical simulations and it has been demonstrated that the energy generated for typical wind speed profiles is greater than that of a traditional control based on a model-based loss minimisation.

Nomenclature

u_{sd}, u_{sq} = stator voltage components in *dq* reference frame
u_{rd}, u_{rq} = rotor voltage components in *dq* reference frame
i_{sd}, i_{sq} = stator current components in *dq* reference frame
i_{rd}, i_{rq} = rotor current components in *dq* reference frame
ψ_{sd}, ψ_{sq} = stator flux linkage components in *dq* reference frame
ψ_{rd}, ψ_{rq} = rotor flux linkage components in *dq* reference frame
θ_s, θ_m = reference frame, rotor position
ω_s, ω_m = reference frame, shaft angular speed
r_s, r_r = stator, rotor resistance per phase
L_s, L_r, L_m = stator, rotor, mutual inductance per phase
P_s, Q_s = stator active and reactive powers
T_{em}, T_m = electromagnetic and mechanical torques
ρ = air density
R = turbine radius
ω_t = turbine angular speed

1 Introduction

Wind energy is one of the most attractive renewable energy for ist large availability and high power density [x]. A wind energy conversion system (WECS) converts the kinetic energy of wind into electrical energy with a wind turbine, an electrical generator and a controller. A gearbox and a converter are optional parts that depend on the type of generator and controller in the WECS.

The efficiency of WECSs has become an interesting research topic over the recent years for the significant potential of reducing of need of fossil fuels for power generation [1, 2]. Variable-speed wind turbines (VSWTs) have being developed to improve the amount of power extracted from wind for all wind speeds and, hence, they are more efficient than fixed-speed wind turbines (FSWTs) [3,4,5]. In a VSWT system, a DFIG is used to convert mechanical power into electrical power as they require only a small power converter in comparison to a permanent magnet synchronous generator.

The maximum mechanical power that can be extracted from a wind turbine is shown in Fig. 1 as a function of the wind speed [6]. In regions 1 and 4, the wind turbine must be halted because the power from the wind turbine is either not enough to sustain a continuous generation or is dangerous for the blades. In region 2, i.e. from cut-in speed, v_{cut-in}, to rated wind speed,v_{rated}, VSWT is controlled with a maximum power point tracking (MPPT) controller. Well-known MPPT methods have been reported in the literature, such as the optimal tip speed ratio (TSR) control [7], the power signal feedback (PSF) control [8], and the perturb and observe (P&O) control [9, 10]. Above the rated speed and up to the cut-out speed, $v_{cut-out}$, the power is limited by either a passive stall control or an active stall with speed control [11] and pitch control [1].

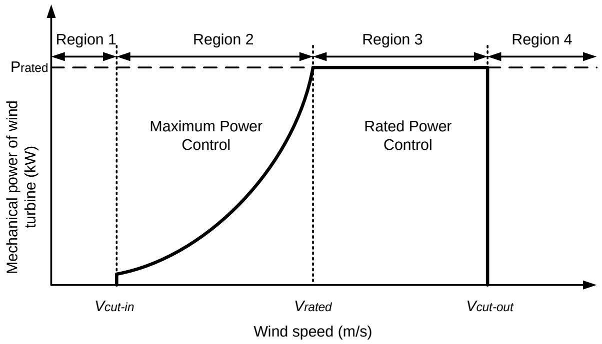

Fig.1: Mechanical power captured from wind turbine [6]

As reported in the literature, pitch control is expensive and has a high maintenance cost [12]. To improve the dynamic efficiency, it is preferable to use a fixed-pitch wind turbine with an active stall control, also known as soft-stalling control, obtained with the speed control of the generator [11, 13, 14]. However, there is still not a clear understanding on the control of fixed-pitch wind turbines for the entire wind speed range indicated in Fig. 1.
MPPT and minimum electric loss (MEL) controllers have been proposed to optimised the efficiency of the wind turbine when the electrical generator is a squirrel-cage induction generator [15, 16]. This control can be extended to DFIGs, with the advantage of independent control of the shaft speed/torque and stator reactive power when a stator field oriented (SFO) vector control of the rotor converter is used [17]. When a DFIG is used as a generator, the efficiency of the WECS can be also improved with an optimal control of the reactive power. Several methods have been proposed to derive the optimal control law of DFIGs, e.g., using a copper loss model [18, 19], an iron and copper loss model [20, 21], and a loss model of the generator, the filter and the power converter [22]. However, all these loss minimisation controllers require the accurate knowledge of the parameters of the DFIG, the filter and the power converter for generating the optimal control law. In practical applications, these parameters are only roughly known and some of them, like the rotor resistance, are sensibly dependent on the temperature [x]. This problem leads to inaccurate determination of the condition of minimum losses, reducing the efficacy of the algorithms.
Searching methods have been used to overcome the limitations of model-based loss minimisation control (MBLC). Several search techniques have been reported in the literature, such as perturb and observe (P&O), genetic algorithm (GA) and particle swam optimisation (PSO) [23].. In this paper, a PSO control is used to maximise the electrical power of DFIG under uncertainty conditions of the DFIG parameters. PSO is one of most efficient meta-heuristics conceptualised from the pattern movement of a flock of bird looking for food to solve optimisation problem [23]. As population-based search algorithm properties, PSO gives the high performance to avoid trapping in its local solution of multi-peak functions.
Therefore, this paper proposes a new optimal control that uses MPPT and a soft-stalling controller to obtain the optimal speed reference for the electrical generator and a PSO searching control to obtain the optimal i_{rd} reference for the SFO vector control.

2 System modelling and description of control

2.1 Wind turbine modelling

The mechanical power extracted from a wind turbine is given by the following expression [x]:

$$P_m = \frac{1}{2}\rho\,\pi\,R^2\,V_w^3\,C_p(\lambda,\beta) \tag{1}$$

The power coefficient of the wind turbine (C_p) is a function of the tip-speed ratio (λ) and the pitch angle (β) and is defined by manufacturer design. In this paper, the power coefficient is given by the approximate formula suggested in [25]:

$$C_p(\lambda,\beta) = 0.5176\left(\frac{116}{\lambda_i} - 0.4\beta - 5\right)e^{-\frac{21}{\lambda_i}} + 0.0068\,\lambda \tag{2}$$

Where:

$$\frac{1}{\lambda_i} = \frac{1}{\lambda + 0.08\beta} - \frac{0.035}{1+\beta^3} \tag{3}$$

The tip-speed ratio can be calculated as:

$$\lambda = \frac{\omega_t R}{V_w} \tag{4}$$

2.2 Doubly-fed induction generator modelling

The three-phase dynamic model of the DFIG in the *d*-*q* reference frame can be expressed by the following equations [17]:

$$\begin{cases} u_{sd} = r_s i_{sd} + \dfrac{d\psi_{sd}}{dt} - \omega_s \psi_{sq} \\ u_{sq} = r_s i_{sq} + \dfrac{d\psi_{sq}}{dt} + \omega_s \psi_{sd} \\ u_{rd} = r_r i_{rd} + \dfrac{d\psi_{rd}}{dt} - (\omega_s - n_p\omega_m)\psi_{rq} \\ u_{rq} = r_r i_{rq} + \dfrac{d\psi_{rq}}{dt} + (\omega_s - n_p\omega_m)\psi_{rd} \\ J\dfrac{d\omega_m}{dt} = T_{em} - T_{load} \end{cases} \tag{5}$$

Under the assumption of negligible iron loss and unsaturated main magnetic circuit, the flux linkage equations, are:

$$\begin{cases} \psi_{sd} = L_s i_{sd} + L_m i_{rd} \\ \psi_{sq} = L_s i_{sq} + L_m i_{rq} \\ \psi_{rd} = L_m i_{sd} + L_r i_{rd} \\ \psi_{rq} = L_m i_{sq} + L_r i_{rq} \end{cases} \tag{6}$$

in which:

$$\begin{aligned} L_s &= L_{ls} + L_m \\ L_r &= L_{lr} + L_m \end{aligned} \tag{7}$$

The equation of the electromagnetic torque is:

$$T_{em} = \frac{3}{2} n_p \frac{L_m}{L_s} \left(\psi_{sq} i_{rd} - \psi_{sd} i_{rq} \right) \tag{8}$$

The stator active and reactive powers are:

$$\begin{cases} P_s = \frac{3}{2} \left(u_{sq} i_{sq} + u_{sd} i_{sd} \right) \\ Q_s = \frac{3}{2} \left(u_{sq} i_{sd} - u_{sd} i_{sq} \right) \end{cases} \tag{9}$$

2.3 Field oriented control of rotor side converter

In the stator flux-oriented control, the *d*-axis of *d*-*q* reference frame is oriented with the stator-flux vector. Therefore, the *dq* components of stator flux linkage are:

$$\begin{aligned} \psi_{sd} &= |\psi| \\ \psi_{sq} &= 0 \end{aligned} \tag{10}$$

Assuming the stator flux linkage constant and neglecting the stator resistance, the stator voltage equations (5) are simplified as:

$$\begin{aligned} u_{sd} &= 0 \\ u_{sq} &= \omega_s \psi_{sd} \end{aligned} \tag{11}$$

Combining (10) and (6), the mechanical equation can be expressed as follows:

$$J \frac{d\omega_m}{dt} = -\frac{3}{2} n_p \frac{L_m}{L_s} \psi_{sd} i_{rq} - T_L \tag{12}$$

and the active and the reactive powers are:

$$\begin{cases} P_s = -\frac{3}{2} \frac{L_m}{L_s} u_{sq} i_{rq} \\ Q_s = \frac{3}{2} \frac{\psi_{sd}}{L_s} u_{sq} - \frac{3}{2} \frac{L_m}{L_s} u_{sq} i_{rd} \end{cases} \tag{13}$$

Equation (12) and (13) point out thatthe electromagnetic torque and the stator active power are controlled only by i_{rq}, while the stator reactive power is controlled only by i_{rd}. Therefore, the control of shaft speed and stator reactive power of the outer control loop can be decoupled by controlling independently i_{rd} and i_{rq}.

3 Optimised control of DFIG for fixed-pitch wind turbines

3.1 MPPT controller

To track maximum power from wind turbine, MPPT controller is used to keep coefficient power C_p at its maximum value, C_{pmax}, when wind speed is below the rated value. From (1), the maximum mechanical power as a function of the turbine shaft speed is:

$$P_{m,opt} = \frac{1}{2} \rho \, \pi \, R^5 \frac{C_{p\max}}{\lambda_{opt}^3} \omega_t^3 = K_{opt} \, \omega_t^3 \tag{14}$$

This paper uses a MPPT algorithm based on PSF for the fast tracking characteristics and simplicity, as it does not need speed sensors. The mechanical power is derived by an observer and, hence, the optimal speed reference is calculated from (15):

$$\omega_{opt}^* = \sqrt[3]{\frac{P_m}{K_{opt}}} \tag{15}$$

3.2 Soft-stalling controller

When the wind speed is higher than the rated value, soft-stalling control is used to limit the power of the turbine to the rated value, P_{mN}, by decreasing the speed of generator down to the stall region. For smooth control between MPPT and soft-stalling, the soft-stalling control is designed a PI controller [13]. This controller provides the compensation terms to subtract from rated speed value, ω_{rN}, to achieve stall operations. The overall block diagram of MPPT and soft-stalling controller is shown in Fig. 2.

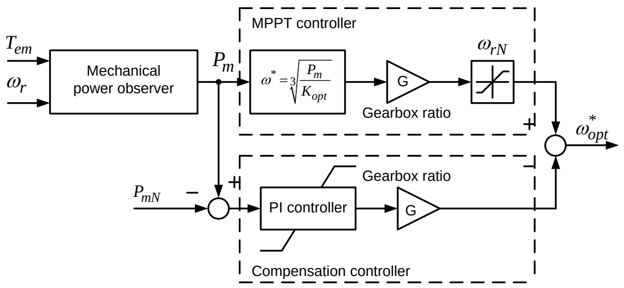

Fig.2: Block diagram of PSF-MPPT and soft-stalling control

3.3 Optimum point tracking of *d*-axis rotor current

Usually, the *d*-axis rotor current of the rotor side converter is regulated to keep the stator reactive power, Q_s, at zero. Withthis strategy, the grid side converter does not have to compensate for the reactive power of the machine. However, the *d*-axis rotor current corresponding to zero stator reactive power is high and, hence, causes additional copper losses in the rotor winding that is undesired [21]. An optimal tracking of the *d*-axis rotor current is provided in this paper to minimise copper losses of DFIG.

3.3.1 Model-based loss minimisation control

To achieve minimum copper losses, the optimal *d*-axis rotor current can be calculated via the DFIG model [18, 21]. From (5) and (9), the steady-state copper losses of the DFIG are:

$$P_{ss\_cu} = \frac{3}{2} r_s \left(i_{sq}^2 + i_{sd}^2 \right) + \frac{3}{2} r_r \left(i_{rq}^2 + i_{rd}^2 \right) \tag{16}$$

Substituting (6) into (16) yields:

$$\begin{aligned} P_{ss\_cu} = \frac{3}{2} \left(r_r + \frac{L_m^2}{L_s^2} r_s \right) i_{rq}^2 + \frac{3}{2} \frac{\psi_{sd}^2}{L_s^2} r_s \\ - \frac{3 \psi_{sd} L_m r_s}{L_s^2} i_{rd} + \frac{3}{2} \left(r_r + \frac{L_m^2}{L_s^2} r_s \right) i_{rd}^2 \end{aligned} \tag{17}$$

As it has been assumed ψ_{sd} constant, the power losses can be minimised by the following equation:

$$\frac{\partial P_{ss\_cu}}{\partial i_{rd}} = -\frac{3L_m r_s \psi_{sd}}{L_s^2} + 3\left(r_r + \frac{L_m^2}{L_s^2} r_s\right) i_{rd} = 0$$

And, hence, the optimal i_{rd} to minimise copper losses is:

$$i_{rd}^* = \frac{L_m r_s \psi_{sd}}{L_m^2 r_s + L_s^2 r_r} \quad (18)$$

3.3.2 Particle swarm optimisation searching control

In the PSO algorithm, n candidate solutions are called particles, (x_1, $x_2, \ldots,$ x_n). At each iteration, each particle x_i directs to the optimal solution under domination of the best particle in a neighbourhood (x_{gbest}) and the best solution found for each particle so far ($x_{pbest,i}$). Each particle is updated using the following formula:

$$x_i(k+1) + x_i(k) + v_i(k+1) \quad (19)$$

where v_i is the velocity of each particle. The velocity is updated calculated as follows:

$$v_i(k+1) = wv_i(k) + c_1 r_1 \left[x_{pbest,i} - x_i(k) \right] + c_2 r_2 \left[x_{gbest} - x_i(k) \right] \quad (20)$$

Where r_1 and r_2 are random vectors with values between 0 and 1, c_1 and c_2 are learning parameters used as acceleration coefficient and w is the inertia weigh [26].

For the optimum tracking of the d-axis rotor current with PSO, the candidate solutions are:

$$x_i(k) = \left[i_{rd,1}^*, \, i_{rd,2}^*, \, \ldots., i_{rd,n}^* \right] \quad (21)$$

Then, the optimal d-axis rotor current corresponds to maximum electrical power generated by the DFIG; hence, the objective function of PSO is evaluated as:

$$P_e\left(i_{rd,i}^*(k)\right) > P_e\left(i_{rd,i}^*(k-1)\right) \quad (22)$$

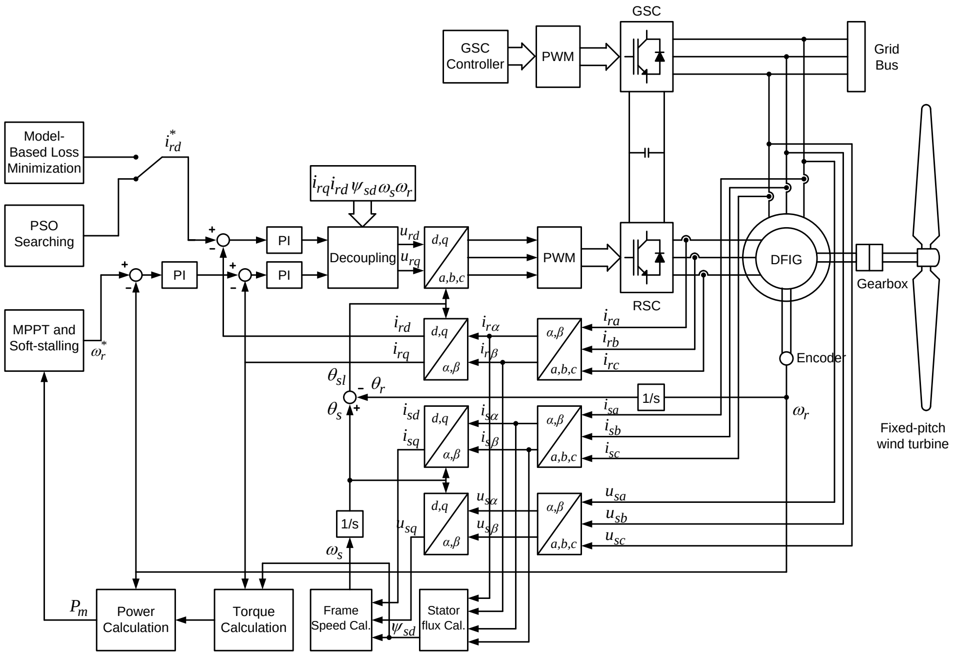

Fig.3: Optimal control block diagram of the WECS based on DFIG

4 Simulation results

The block diagram of the optimal control of the WECS is shown in Fig. 3. The wind turbine is coupled with the DFIG via a gearbox and the DFIG is connected to the busbars of a stiff grid. A back-to-back converter supplies the rotor circuit: the rotor side converter (RSC) controls the generator speed and the stator reactive power, while the grid side converter (GSC) controls the grid reactive power and the DC-link capacitor voltage. The MPPT is used for tracking the maximum mechanical power from the wind, while the reference for the shaft speed is given by the optimisation algorithm. Copper losses of the DFIG are minimised through the control of the d-axis rotor current,.The parameters of the wind turbine and the DFIG used for the simulations are given in Table 1 and 2, respectively.

The proposed optimal control algorithm is verified using Matlab/Simulink to validate its performances incorporating a DFIG model, wind turbine model and vector control. The MPPT and soft-stall controller are applied as per Fig. 2 and pitch angle of turbine is fixed at zero. In order to improve the efficiency of DFIG, the MBLC and PSO algorithm are used to compare performance of results when DFIG parameter values are changed from the parameters given in Table 2. The optimal d-axis rotor current reference of the MBLC is provided by Equation (26). The PSO search is done by its algorithm aforementioned above with 3 d-axis rotor current reference candidates. The parameters of PSO are defined as r_1, r_2 are 0.5, c_1, c_2 are 0.729, 1.494 and w is 0.15, respectively. The sampling period of PSO is chosen as 0.3 seconds.

Parameter	*Value*	*Unit*
Rated power (P_{mN})	5	kW
Blade radius (R)	2.327	m
Gearbox ratio (G)	7	-
Rated wind speed (V_{rated})	10	m/s
Cut-in wind speed ($V_{cut\text{-}in}$)	4	m/s
Cut-out wind speed ($V_{cut\text{-}out}$)	14	m/s
Maximum power coefficient (C_{pmax})	0.48	-
Optimal tip-speed ratio (λ_{opt})	8.1	-
Equivalent moment of inertia (J_T)	0.5	Kgm^2

Table 1: Wind turbine characteristics.

Parameter	*Value*	*Unit*
Synchronous speed	1500	rpm
Rated stator voltage	380	V
Rated stator current	8.36	A
Rated torque	31.8	Nm
Rated rotor voltage	205	V
Stator-rotor turns ratio	0.54	-
Stator resistance (R_s)	720	mΩ
Stator leakage inductance (L_{ls})	5.8	mH
Mutual inductance (L_m)	85.8	mH
Rotor resistance referred to stator phase	750	mΩ
(R_r)	5.8	mH
Rotor leakage inductance referred to	2	-
stator phase (L_{lr})	0.024	Kgm^2
Number of pole pairs (p)		
Inertia (J_G)		

Table 2: DFIG characteristics [16].

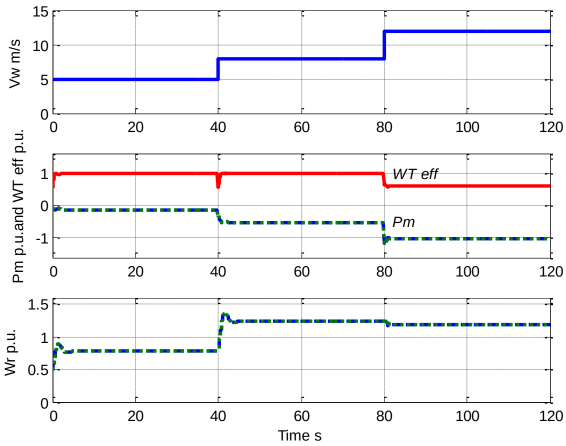

(a)

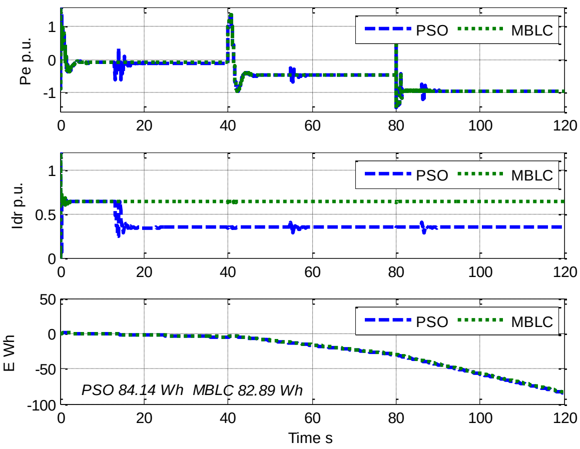

(b)

Fig. 4: Simulation results of proposed control with step changing wind speed from 5 to8 and then from 8 to 12 m/s when the error on the estimation of L_m is -50%.

Fig. 4 and 5 show the performance of the proposed control system when the wind speed changes as a step every 40 seconds and the mutual inductance of DFIG is uncertain and the control uses a value smaller than 50% of the real one in Table 2. The simulations show that the MPPT control based on PSF and soft-stalling has adequate performance in the entire speed range as shown in Fig. 4(a) and 5(a). The speed variation is limited by the inertia of the wind turbine and the generator and, as such, the performance would be affected when the wind speed has high rate of variation. The simulations in Fig. 4(b) and 5(b) also compare PSO and MBLC in terms of electrical power and energy. The figures show that the energy generated by PSO is slightly higher than that of MBLC in both cases. Also, it can be observed that the proposed control gives smoother generator speed trajectory between the MPPT and soft-stalling controller for both step-up and step-down change of wind speed, i.e. at 80 seconds in Fig. 4 and 40 seconds in Fig. 5.

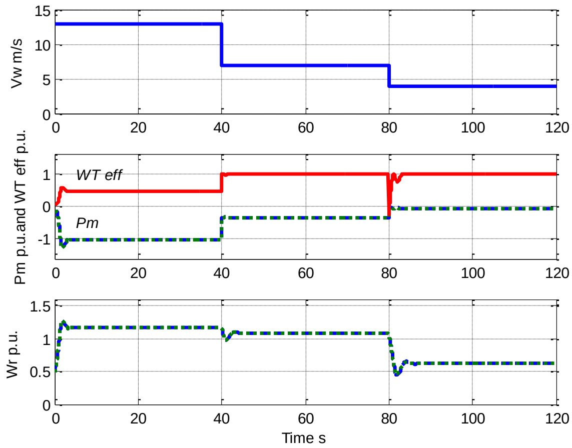

(a)

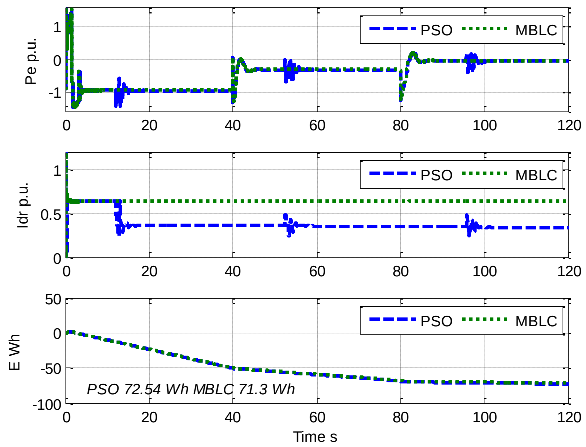

(b)

Fig. 5: Simulation results of the proposed control with step-changing wind speed from 13 to 7 and from 7 to 4 m/s when the error on the estimation of L_m is -50%.

DFIG Parameter variations of Model-Based Method	*Extra energy extracted from PSO*
Variation of -10% of L_m	-0.01%
Variation of -30% of L_m	+0.33%
Variation of -50% of L_m	+1.78%
Variation of +10% of R'_r	-0.01%
Variation of +30% of R'_r	+0.04%
Variation of +50% of R'_r	+0.10%

Table 3: Energy generated by the DFIG with a PSO in comparison with a MBLC with an error in the estimation of machine parameters for a simulation of 2 minute.

The influence on the error in the estimation of DFIG parameters has been analysed in Tab. 3 for a constant wind speed of 8 m/s with reference to L_m and R_r, which are the parameters most likely to be affected by the operating conditions of the machines.. Tab. 3 shows that the error on the estimation of L_m produces a much larger effect than the error on R_r. For example, in case of an error of -50% in the estimation of L_m, the PSO generates 1.78% more energy than MBLC over a period of 2 minutes, i.e. 1 kWh/day extra. [Analyse what those results tells us]

5 Conclusion

This paper proposes a new optimal control of WECS with DFIG for fixed-pitch wind turbines to maximise the mechanical and electrical powers.

The simulations on a sample wind turbine with DFIG show that MPPT based on PSF and soft-stalling and PSO controllers give improved efficiencies for the entire speed range of the turbine. The proposed control also provides smooth generator speed trajectory at the transition from PSF to soft-stalling.

The PSO searching control algorithm provides advantages of robustness of the control against uncertainties on the parameters of the DFIG. The simulations have shown that the rotor speed has to change substantially to follow the variations of the wind speed, but this is limited by the wind turbine inertia. This issue requires further work on the analysis of the control strategy for extremely variable wind speeds, where the torque of the generator could be reversed to improve the dynamical response of the speed control.

Acknowledgements

Authors would like to thank the Thai government for sponsoring the PhD Scholarship of the lead author.

References

[1] Z. Chen, J. M. Guerrero, F. Blaabjerg, and S. Member, “A Review of the State of the Art of Power Electronics for Wind Turbines,” *IEEE Trans. Power Electron.*, vol. 24, no. 8, pp. 1859–1875, 2009.

[2] H. Li and Z. Chen, “Overview of different wind generator systems and their comparisons,” *Renew. Power Gener. IET*, vol. 1, no. 1, pp. 10–16, 2007.

[3] R. Pena, J. C. Clare, and G. M. Asher, “Doubly fed induction generator using back-to-back PWM converters and its application to variable-speed wind-energy generation,” *IEE Proc. - Electr. Power Appl.*, vol. 143, no. 3, p. 231, 1996.

[4] A. Miller, E. Muljadi, and D. S. Zinger, “A variable speed wind turbine power control,” *IEEE Trans. Energy Convers.*, vol. 12, no. 2, pp. 181–186, 1997.

[5] L. Holdsworth, X. G. Wu, J. B. Ekanayake, and N. Jenkins, “Comparison of fixed speed and doubly-fed induction wind turbines during power system disturbances,” *IEE Proc. - Gener. Transm. Distrib.*, vol. 150, no. 3, p. 343, 2003.

[6] D. Kumar and K. Chatterjee, “A review of conventional and advanced MPPT algorithms of wind energy systems,” *Science Direct, Renewable and Sustainable Energy Reviews*, 2016.

[7] S. Cai and H. Wen, “Modeling and MPPT Control of DFIG Wind Energy System,” *Renew. Power Gener. (RPG 2015)*, 2015.

[8] J. S. Thongam, P. Bouchard, R. Beguenane, A. F. Okou, and A. Merabet, “Control of variable speed wind energy conversion system using a wind speed sensorless optimum speed MPPT control method,” *IECON 2011 - 37th Annu. Conf. IEEE Ind. Electron. Soc.*, pp. 855–860, 2011.

[9] J. Yaoqin, Y. Zhongqing, and C. Binggang, “A new maximum power point tracking control scheme for wind generation,” *Int. Conf. Power Syst. Technol.*, pp. 144–148, 2002.

[10] X. Du and H. Yin, “MPPT control strategy of DFIG-based wind turbines using double steps hill climb searching algorithm,” *Proc. 5th IEEE Int. Conf. Electr. Util. Deregulation, Restruct. Power Technol. DRPT 2015*, pp. 1910–1914, 2016.

[11] B. Neammanee, S. Sirisumrannukul, and S. Chatratana, “Control Strategies for Variable-speed Fixed-pitch Wind Turbines,” *Wind Power, Tech*, no. June, pp. 209–

230, 2010.
[12] H. Vihriala, “Control of Variable Speed Wind Turbine,” PhD Thesis, Tempere University of technology, 2002.
[13] C. Jiawei, W. Changyun, and S. Yongduan, “Power control strategy for variable-speed fixed-pitch wind turbines,” *2014 13th Int. Conf. Control Autom. Robot. Vision, ICARCV 2014*, vol. 2014, no. December, pp. 559–564, 1997.
[14] Z. Xin-fang, X. Da-ping, and L. Yi-bing, “Adaptive optimal fuzzy control for variable speed fixed pitch wind turbines,” *5th World Congr. Intell. Control Autom. (IEEE Cat. No.04EX788)*, vol. 3, pp. 2481–2485, 2004.
[15] A. Mesemanolis, C. Mademlis, and I. Kioskeridis, “High-efficiency control for a wind energy conversion system with induction generator,” *IEEE Trans. Energy Convers.*, vol. 27, no. 4, pp. 958–967, 2012.
[16] A. Mesemanolis, C. Mademlis, and I. Kioskeridis, “Optimal efficiency control strategy in wind energy conversion system with induction generator,” *IEEE J. Emerg. Sel. Top. Power Electron.*, vol. 1, no. 4, pp. 238–246, 2013.
[17] G. Abed, J. Lopez, M. A. Rodriguez, L. Marroyo, and G. Iwanski, *DOUBLY FED INDUCTION MACHINE MODELING AND CONTROL FOR WIND ENERGY GENERATION*. John Wiley & Sons, Inc., 2011.
[18] Y. Tang and L. Xu, “A Flexible Active and Reactive Power Control Strategy for a Variable Speed Constant Frequency Generating System,” *IEEE Trans. Power Electron.*, vol. 10, no. 4, pp. 472–478, 1995.
[19] K. Krajangpan, W. Sadara, and B. Neammanee, “Control strategies for maximum active power and minimum copper loss of doubly fed induction generator in wind turbine system,” *2010 Int. Conf. Power Syst. Technol. Technol. Innov. Mak. Power Grid Smarter, POWERCON2010*, pp. 1–7, 2010.
[20] A. G. Abo-Khalil, H. G. Park, D. C. Lee, S. P. Ryu, and S. H. Lee, “Loss Minimization Control for Doubly-Fed Induction Generators in Variable Speed Wind Turbines,” *Annu. Conferr. IEEE Ind. Electron. Soc.*, pp. 1109–1114, 2007.
[21] A. H. Kasem, E. F. El-Saadany, H. H. El- Tamaly, and M. A. A. Wahab, “Performance enhancement of DFIG-based wind turbines close to the rated operation,” *40th North Am. Power Symp. NAPS2008*, pp. 6–11, 2008.
[22] B. Zhang, W. Hu, and Z. Chen, “Loss Minimizing Operation of Doubly Fed Induction Generator Based Wind Generation Systems Considering Reactive Power Provision,” *IEEE Ind. Soc. IECON 2014*, 2014.
[23] J. Kennedy and R. Eberhart, “Particle swarm optimization,” *Neural Networks, 1995. Proceedings., IEEE Int. Conf.*, vol. 4, pp. 1942–1948 vol.4, 1995.
[24] L. Fan and Z. Miao, *Modeling and Analysis of Doubly Fed Induction Generator Wind Energy Systems*. ScienceDirect, 2015.
[25] S. Heier, *Grid Integration of Wind Energy Conversion Systems*, vol. 21. JohnWiley & Sons, Ltd, 2000.
[26] K. Ishaque, Z. Salam, M. Amjad, and S. Mekhilef, “An improved particle swarm optimization (PSO)-based MPPT for PV with reduced steady-state oscillation,” *IEEE Trans. Power Electron.*, vol. 27, no. 8, pp. 3627–3638, 2012.